Supporting Information

Nitrogen-doped, Oxygen-functionalized, Edge- and Defect-rich vertical aligned graphene for high-performance oxygen evolution reaction

Dongqi Li, Bowen Ren, Qiuyan Jin, Hao Cui *, Chengxin Wang*

State Key Laboratory of Optoelectronic Materials and Technologies, School of Materials Science and Engineering, Sun Yat-sen University, Guangzhou 510275, China

The Key Laboratory of Low-Carbon Chemistry & Energy Conservation of Guangdong Province, Sun Yat-sen University, Guangzhou 510275, China

*Corresponding author: Fax: +86-20-8411-3901; e-mail: wchengx@mail.sysu.edu.cn; cuihao3@mail.sysu.edu.cn.

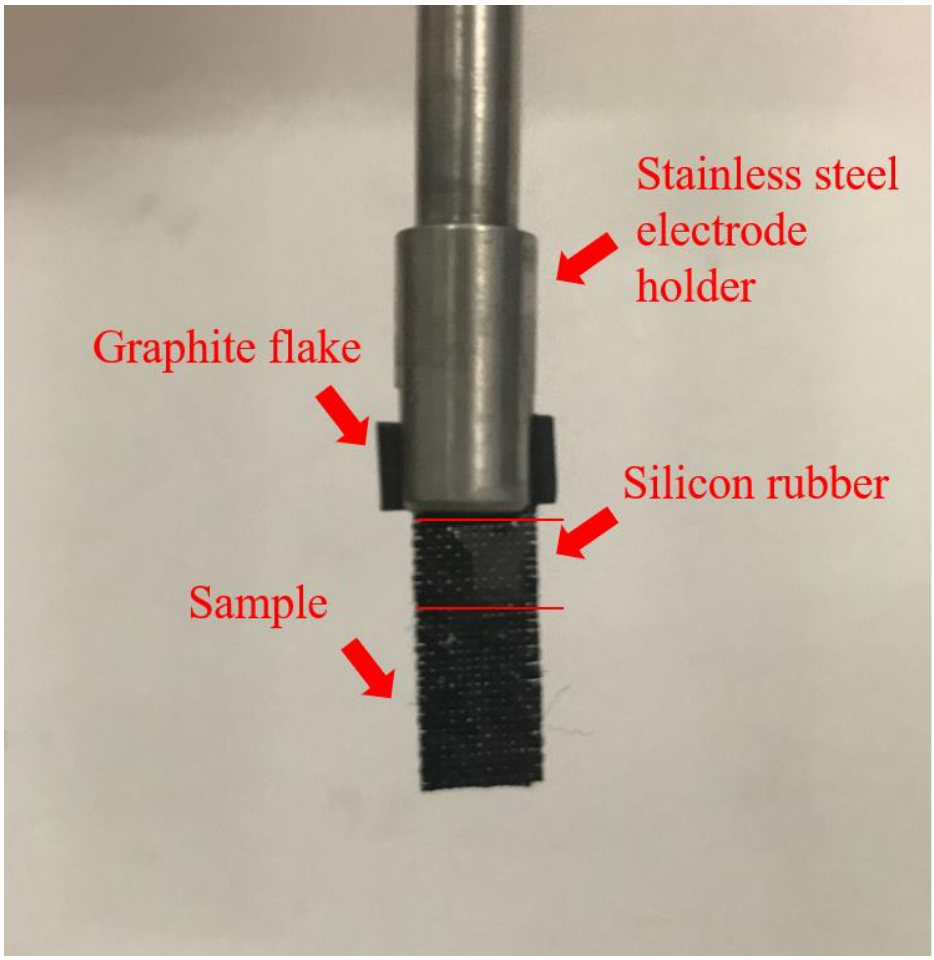

Fig. S1. The optical photograph of working electrode.

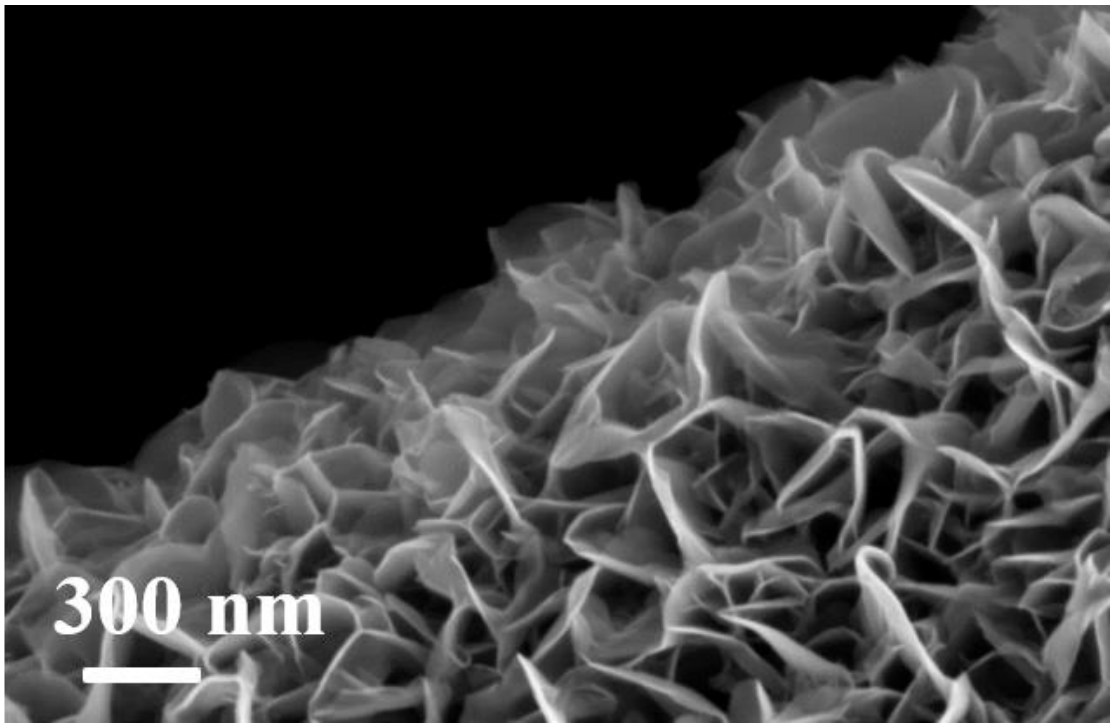

Fig. S2. The SEM images of the side view of N, O-VAGNs/CC.

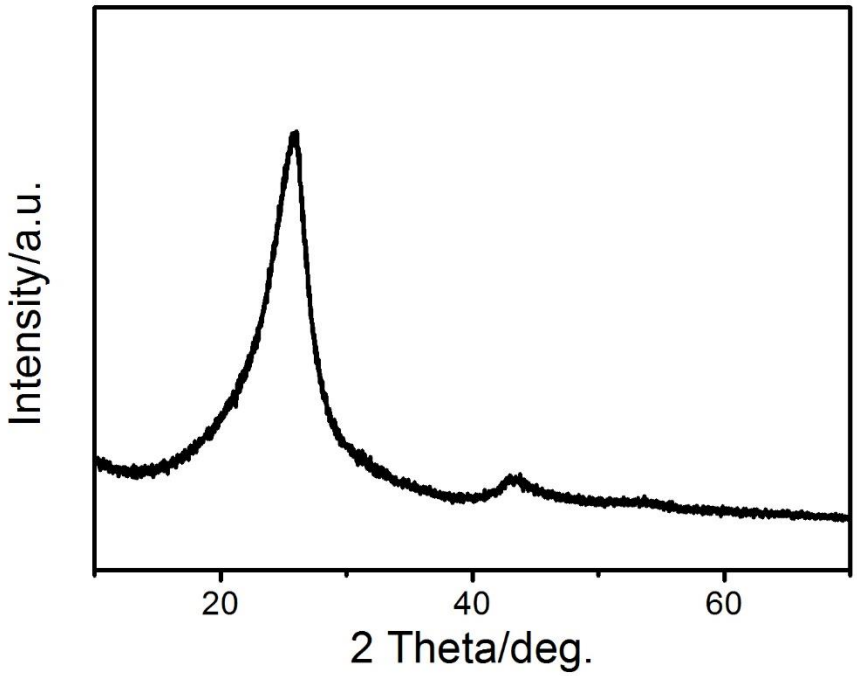

Fig. S3. The XRD pattern of N, O-VAGNs/CC.

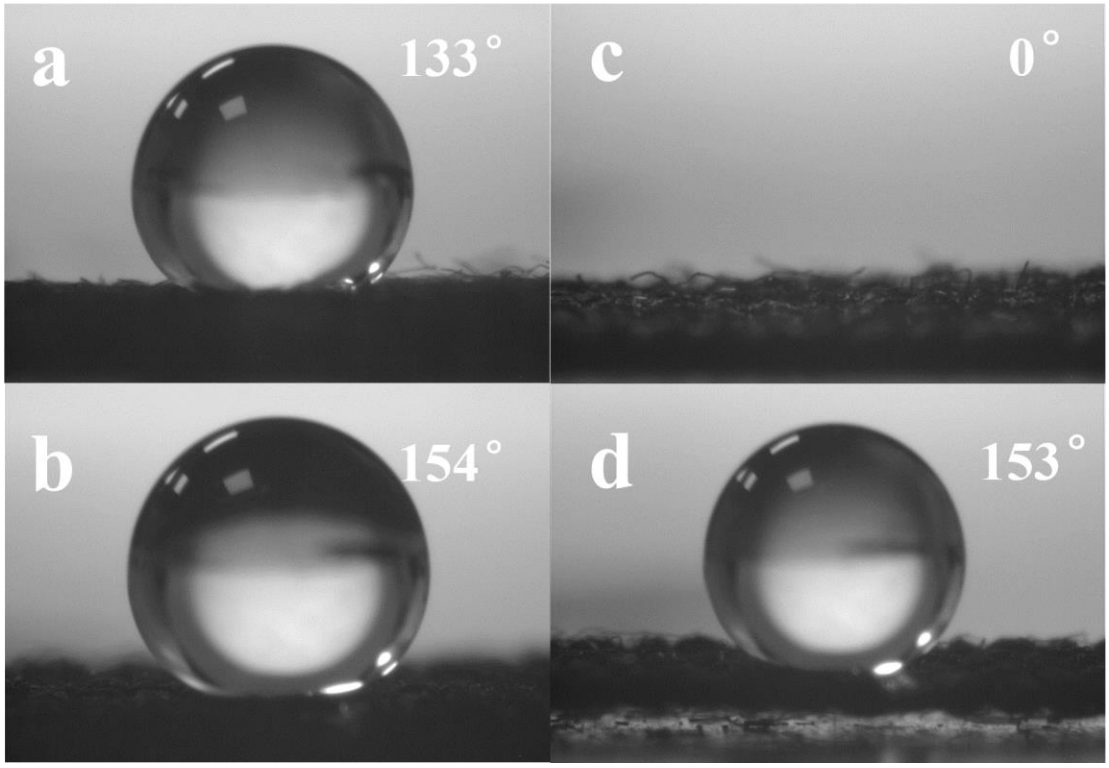

Fig. S4. The water contact angle of N, O-VAGNs/CC and VAGNs/CC brfore (a, b) and after (c, d) activation.

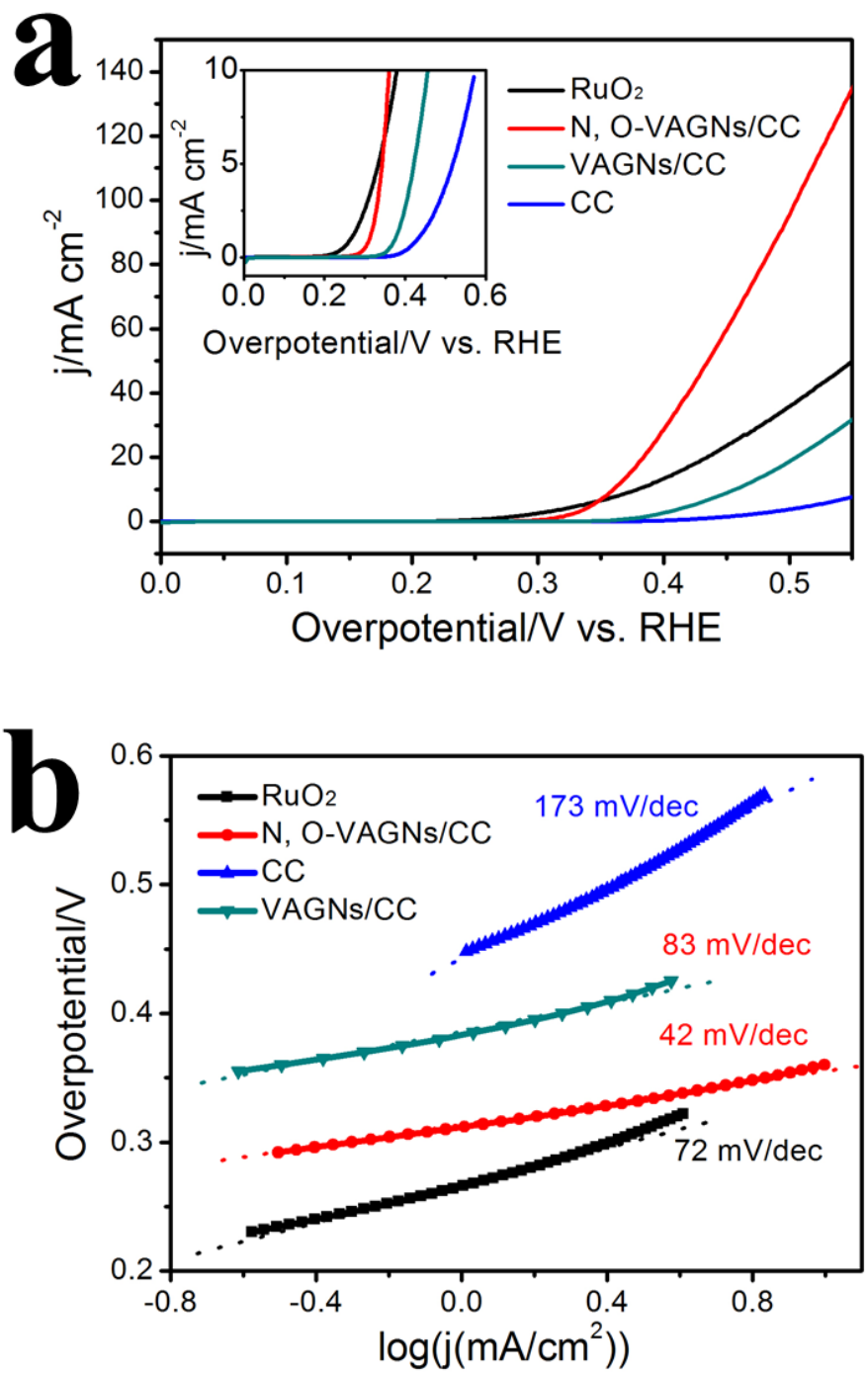

Fig. S5. The (a) Polarization curves with its corresponding (b) Tafel plots of N, O-VAGNs/CC, VAGNs/CC, RuO_2 and CC, and the LSV data were presented without iR compensation.

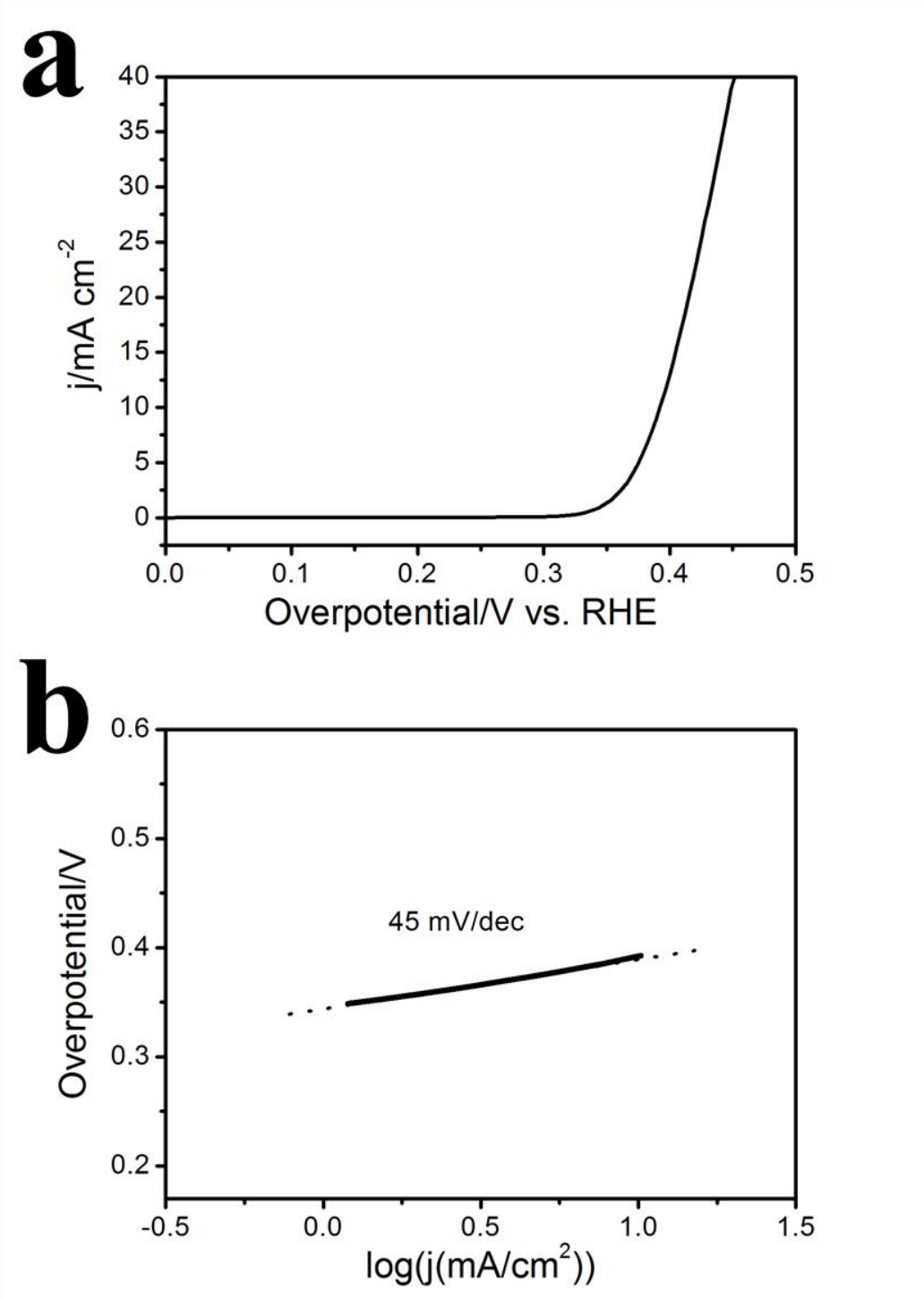

Fig. S6. The (a) Polarization curves with its corresponding (b) Tafel plots of N, O-VAGNs/CC measured in 0.1 M KOH. In this measurements, Hg/HgO electrode (0.0977V vs RHE) and graphite rod were used as reference electrode and counter electrode, respectively. The reference electrode was calibrated to be 0.866V in 0.1 M KOH with respect to a reversible hydrogen electrode (RHE).

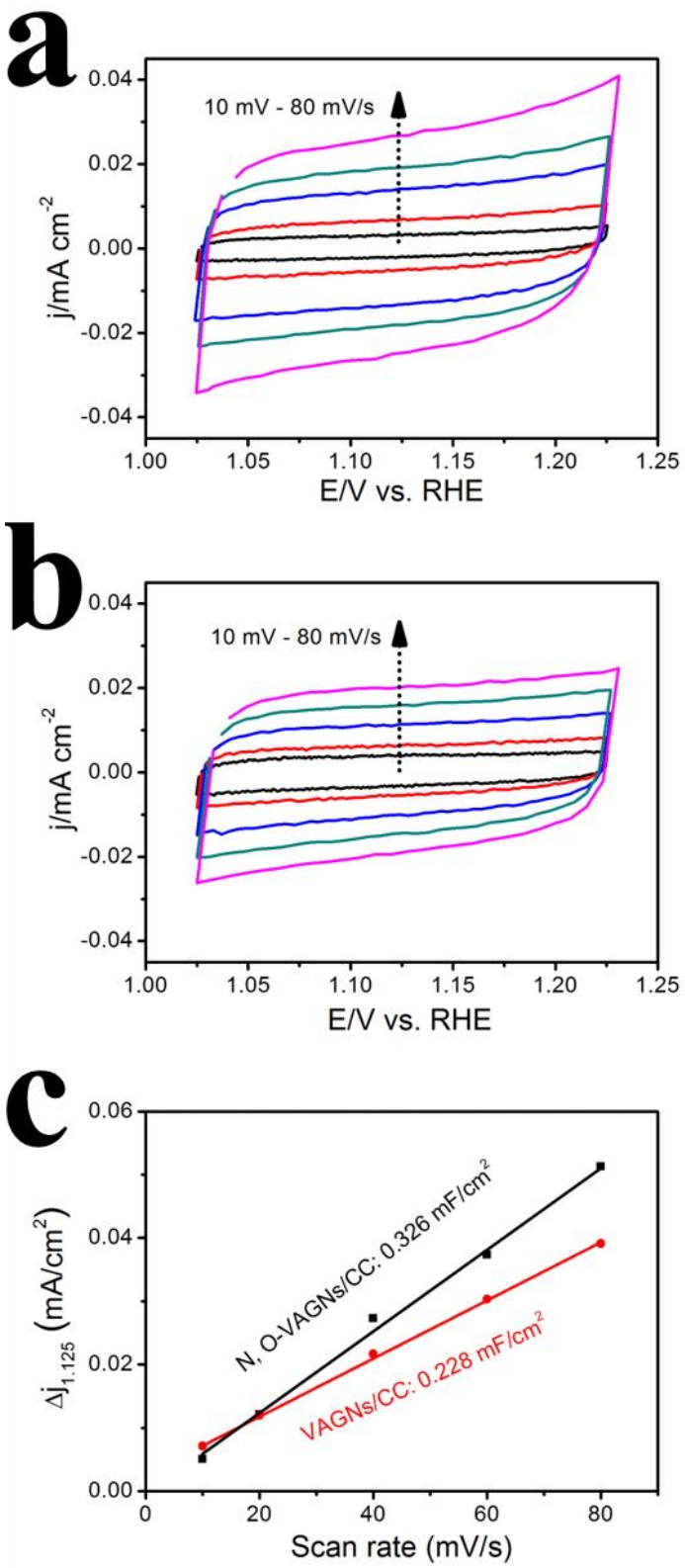

Fig. S7. The cyclic voltammograms with the scan rate of 10, 20, 40, 60, 80 mV/s within 1.025 to 1.225 V of (a) N, O-VAGNs/CC, (b) VAGNs/ CC and (c) its corresponding double-layer charging current density difference ($\Delta j = j_a - j_c$) at 1.125 V ploted against scan rate of N, O-VAGNs/CC and VAGNs/CC.

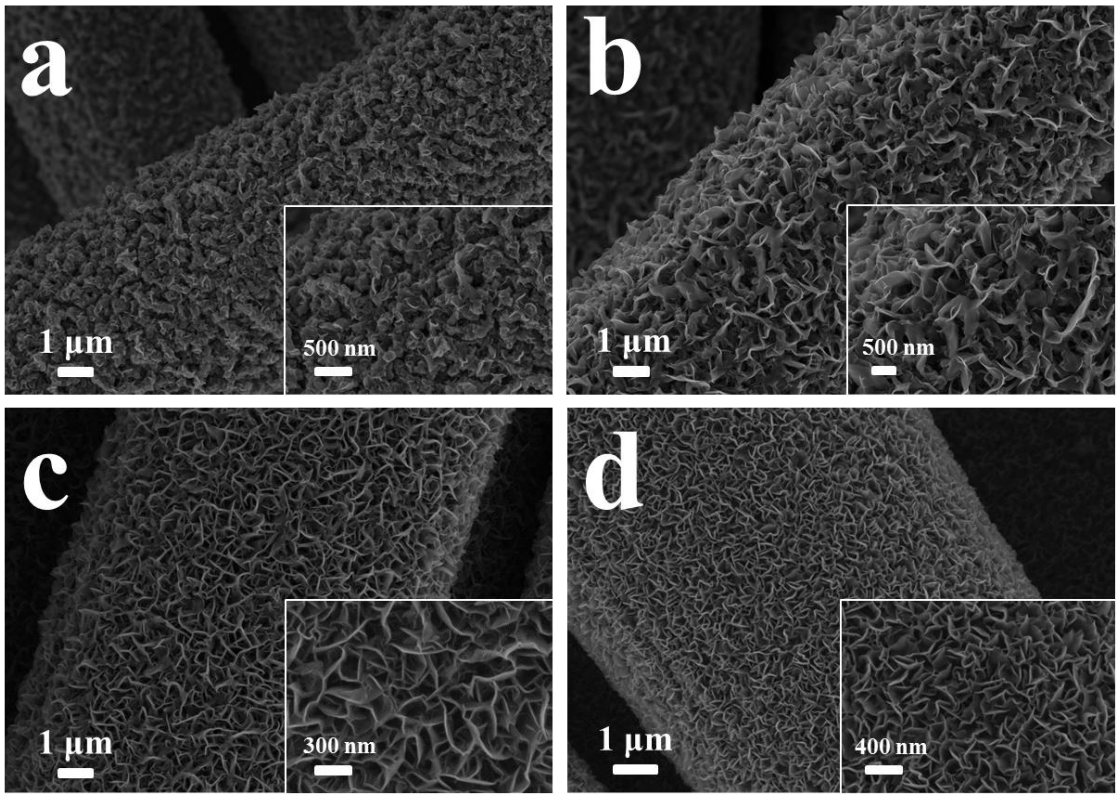

Fig. S8. The low- and high-magnification (inset) SEM images of (a) N, O-VAGNs/CC-1:2, (b) N, O-VAGNs/CC-1:1, (c) N, O-VAGNs/CC-2:1 and (d) N, O-VAGNs/CC-4:1.

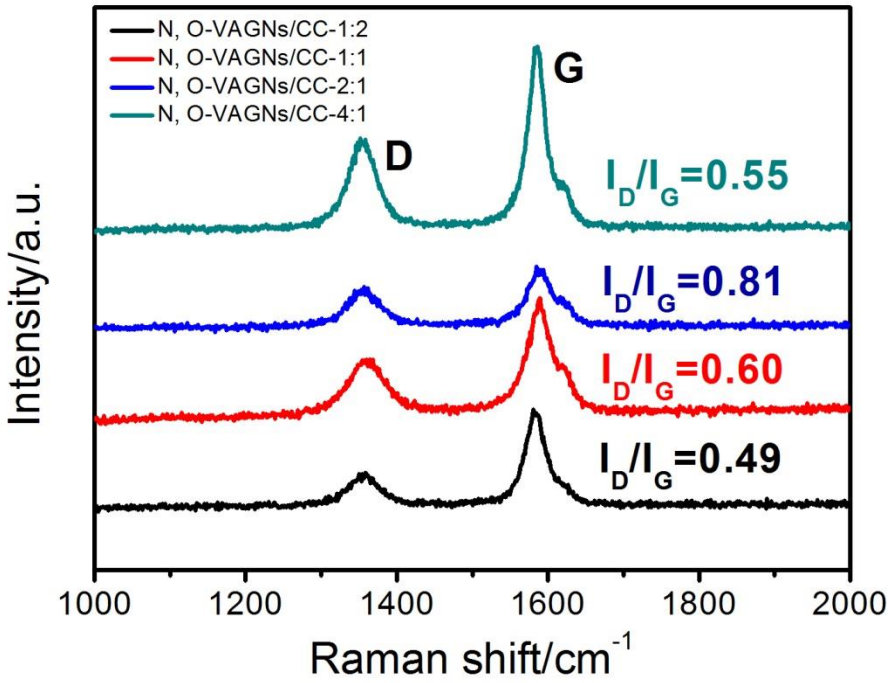

Fig. S9. The Raman spectroscopy of N, O-VAGNs/CC-1:2, N, O-VAGNs/CC-1:1, N, O-VAGNs/CC-2:1 and N, O-VAGNs/CC-4:1.

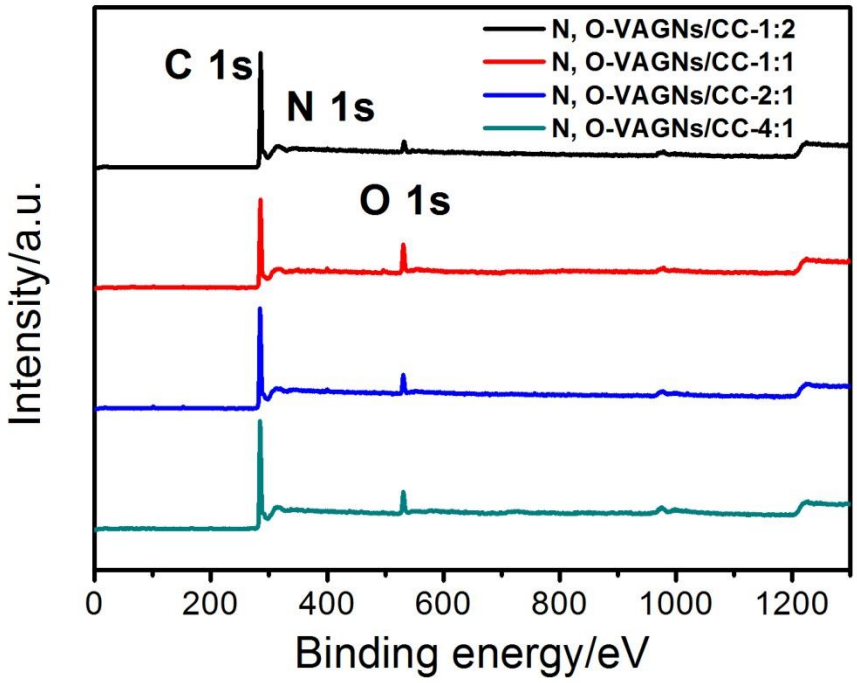

Fig. S10. The XPS survey spectra of N, O-VAGNs/CC-1:2, N, O-VAGNs/CC-1:1, N, O-VAGNs/CC-2:1 and N, O-VAGNs/CC-4:1.

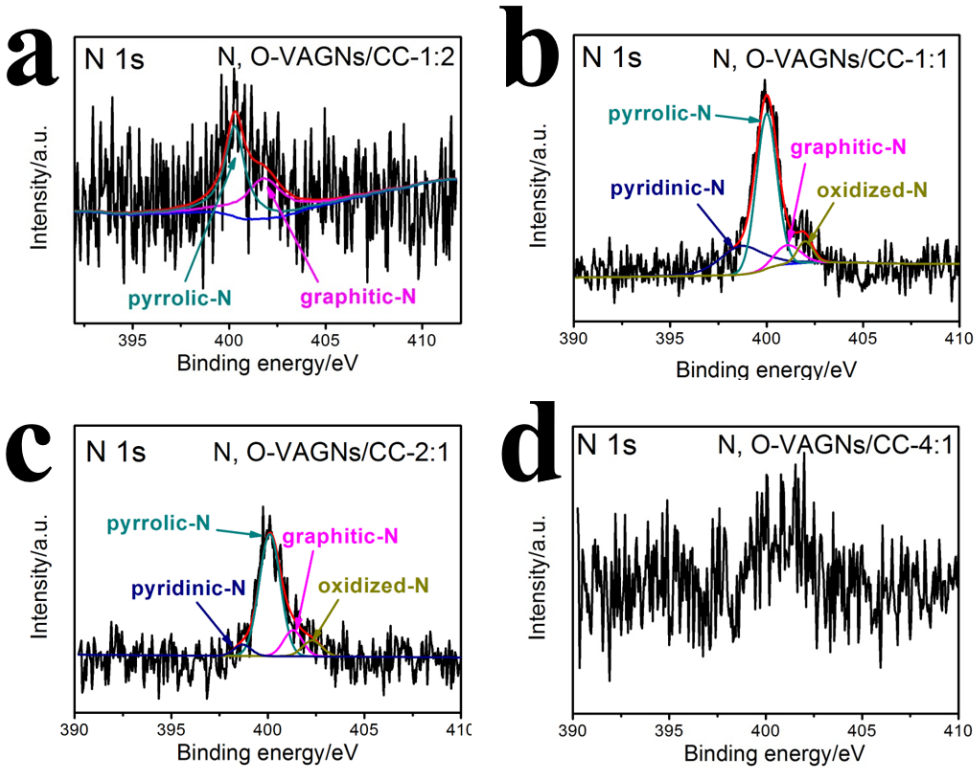

Fig. S11. The high resolution XPS spectra in N 1s region of (a) N, O-VAGNs/CC-1:2, (b) N, O-VAGNs/CC-1:1, (c) N, O-VAGNs/CC-2:1 and (d) N, O-VAGNs/CC-4:1.

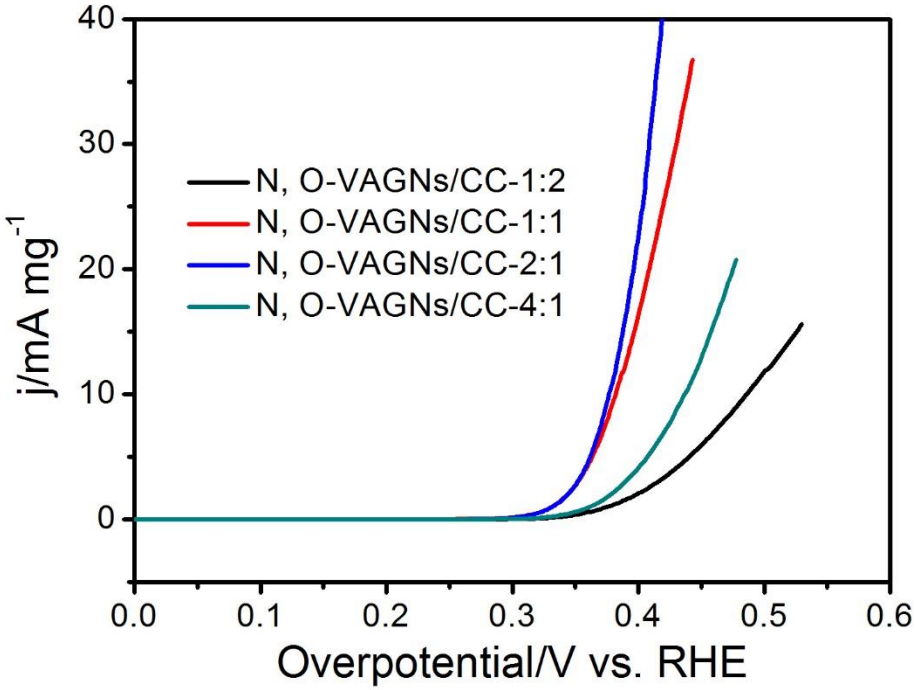

Fig. S12. The loading-normalized current density.

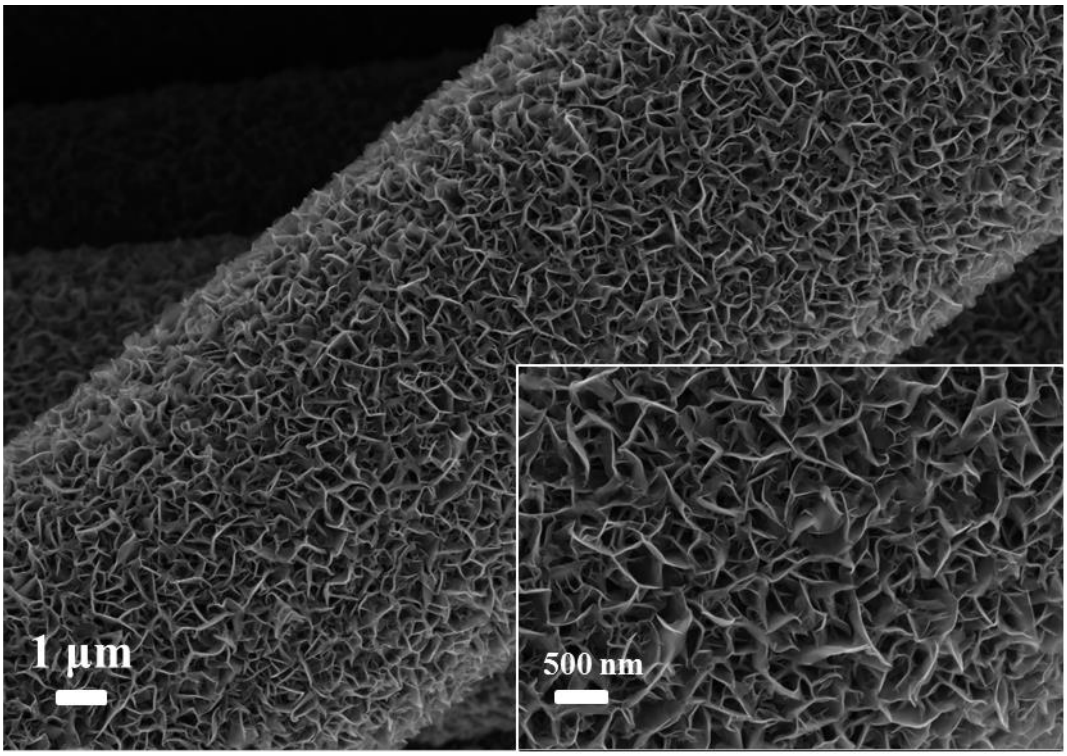

Fig. S13. The SEM images of N, O-VAGNs/CC after the long-term durability measurement.

Table S1. The specific contents of C, N and O in the samples of N, O-VAGNs/CC and VAGNs/CC ("-" indicates that the element is not exist in the samples).

Sample	N, O-VAGNs/CC	VAGNs/CC
Total content of C (at %)	89.1	99.01
Total content of N (at %)	2.05	-
Total content of O (at %)	8.86	0.99

Table S2. The percentage composition for sp^2, sp^3, C-O, C-N, C=O and O-C=O in the samples of N, O-VAGNs/CC and VAGNs/CC ("-" indicates that the groups are not exist in the samples).

sample	sp^2	sp^3	C-O, C-N	C=O	O-C=O
N, O-VAGNs/CC (at %)	71.01	13.61	5.23	5.51	4.64
VAGNs/CC (at %)	80.9	10.37	5.05	-	3.68

Table S3. Elemental analysis of N. This test was carried by the elemental analyzer (vario EL cube).

Sample	Weight (mg)	N (%)
VAGNs/CC	1.593	0
N, O-VAGNs/CC	1.466	0.21
CC	2.07	0

Table S4. The percentage composition for different chemical states of N in the samples of N, O-VAGNs/CC and VAGNs/CC ("-" indicates that groups are not exist in the samples).

sample	Pyridinic-N	Pyrrolic-N	Graphitic-N	oxidized-N
N, O-VAGNs/CC (at %)	6.52	70.20	14.90	8.38
VAGNs/CC (at %)	-	-	-	-

Table S5. The percentage composition for different chemical states of O in the samples of N, O-VAGNs/CC and VAGNs/CC.

sample	COO^- and O=C-O	C-OH and C=O	O=C-O
N, O-VAGNs/CC (at %)	72.68	17.99	9.33
VAGNs/CC (at %)	13.86	57.22	28.92

Table S6. The comparison of the onset potential, η_{10} and Tafel slope of N, O-VAGNs/CC in this work and other carbon-based OER electrocatalysts ("~" means that the values are our estimation based on the reported data; "-" indicates that the values are not able to be extracted from the reported papers).

Materials	**Onset potential (mV)**	**Overpotential at 10 mA cm^{-2} (mV)**	**Tafel slop (mV/dec)**	**Reaction solution**	**Ref.**
N, O-VAGNs/CC	269	351	38	1 M KOH	This work
	344	390	45	0.1 M KOH	
P-doped graphene	250	330	62	1 M KOH	S1
N, F-doped graphene	220	340	78	1 M KOH	S2
Porous carbon cloth	-	360	98	1 M KOH	S3
O, N, P tri-doped graphite nanocarbon	~320	410	84	1 M KOH	S4
O-doped graphene	-	450	-	1 M KOH	S5
N, O-dual doped graphene with nanotubes	315	~500	141	0.1 M KOH	S6
Nanoporous carbon nanofiber films	200	~620	274	0.1 M KOH	S7
N, P, F tri-doped graphene	390	~570	136	0.1 M KOH	S8
RuO_2	265	379	56	1 M KOH	This work
Ni/Mo_2C	270	368	-	1 M KOH	S9
FeP nanoparticles	250	320	50	1 M KOH	S10
CoNPs@C	140	270	59	1 M KOH	S11
Co@Co_3O_4/NC	350	410	-	0.1 M KOH	S12

Table S7. The specific content of C, N and O in the samples of N, O-VAGNs/CC-1:2, N, O-VAGNs/CC-1:1, N, O-VAGNs/CC-2:1 and N, O-VAGNs/CC-4:1.

Sample	N, O-VAGNs/CC-1:2	N, O-VAGNs/CC-1:1	N, O-VAGNs/CC-2:1	N, O-VAGNs/CC-4:1
Total content of C (at %)	93.71	83.15	89.1	91.9
Total content of N (at %)	0.87	3.44	2.05	0.7
Total content of O (at %)	5.41	13.41	8.86	6.4

Table S8. The loading amounts of different samples prepared by various flow ratio of CH_4:N_2 in MPECVD system as 1:2, 1:1, 2:1 and 4:1. (Corresponding to N, O-VAGNs/CC-1:2, N, O-VAGNs/CC-1:1, N, O-VAGNs/CC-2:1 and N, O-VAGNs/CC-4:1). The loading amount of these samples were tested by an Ultra-Microbalances (Mettler Toledo XP2U).

CH_4:N_2	1:2	1:1	2:1	4:1
Loading amount (mg/cm^2)	3.1713	3.2849	3.5900	3.9053

Reference

[S1] Z. Xiao, X. Huang, L. Xu, D. Yan, J. Huo, S. Wang, *Chem. Commun.*, 2016, 52, 13008-13011.

[S2] X. Yue, S. Huang, J. Cai, Y. Jin, P. K. Shen, *J. Mater. Chem. A*, 2017, 5, 7784-7790.

[S3] M. S. Balogun, W. Qiu, H. Yang, W. Fan, Y. Huang, P. Fang, G. Li, H. Ji, Y. Tong, *Energy Environ. Sci.*, 2016, 9, 3411-3416.

[S4] J. Lai, S. Li, F. Wu, M. Saqib, R. Luque, G. Xu, *Energy Environ. Sci.*, 2016, 9, 1210-1214.

[S5] Z. Liu, Z. Zhao, Y. Wang, S. Dou, D. Yan, D. Liu, Z. Xia, S. Wang, *Adv. Mater.*, 2017, 29, 1606207.

[S6] S. Chen, J, Duan, M. Jaroniec, S. Z. Qiao, *Adv. Mater.*, 2014, 26, 2925-2930.

[S7] Q. Liu, Y. Wang, L. Dai, J. Yao, Adv. Mater., 2016, 28, 3000-3006.

[S8] J. Zhang, L. Dai, *Angew. Chem. Int. Ed.*, 2016, 55, 13296-13300.

[S9] Z. Y. Yu, Y. Duan, M. R. Gao, C. C. Lang, Y. R. Zheng, S. H. Yu, *Chem. Sci.*, 2017, 8, 968-973.

[S10] J. Masud, S. Umapathi, N. Ashokaan, M. Nath, *J. Mater. Chem. A*, 2016, 4, 9750-9754.

[S11] Q. Y. Jin, B. W. Ren, D. Q. Li, H. Cui, C. X. Wang, *ACS Appl. Mater. Interfaces*, 2017, 9, 31913-31921.

[S12] A. Aijaz, J. Masa, C. Rosler, W. Xia, P. Weide, A. J. R. Botz, R. A. Fischer, W. Schuhmann, M. Muhler, *Angew. Chem.*, 2016, 128, 4155-4160.